Do CMIP5 models reproduce observed low-frequency North Atlantic jet variability?

Thomas J. Bracegirdle[1], Hua Lu[1], Rosie Eade[2], Tim Woollings[3]

[1]British Antarctic Survey, Cambridge, UK.

[2]Met Office Hadley Centre, Exeter, UK

[3]Department of Physics, Atmospheric, Oceanic and Planetary Physics, University of Oxford, Oxford, UK

Corresponding author: Thomas J. Bracegirdle (tjbra@bas.ac.uk)

Key Points:

- Reproducing post-1862 N Atlantic (NA) multi-decadal jet strength variability is a tougher test for models than reproducing NAO variability
- An observed strong multi-decadal correlation between NA jet strength and NAO may be specific to the 1862-2005 period.
- Efforts to improve models' representation of NA low-frequency variability should involve understanding drivers of jet strength variability.

Abstract

The magnitude of observed multi-decadal variations in the North Atlantic Oscillation (NAO) is at the upper end of the range simulated by climate models and a clear explanation for this remains elusive. Recent research shows that observed multi-decadal NAO variability is more strongly associated with North Atlantic (NA) jet strength than latitude, thus motivating a comprehensive comparison of NA jet and NAO variability across the CMIP5 models. Our results show that the observed peak in multi-decadal jet strength variability is even more unusual than NAO variability when compared to the model-simulated range across 133 historical CMIP5 simulations. Some CMIP5 models appear capable of reproducing the observed low-frequency peak in jet strength, but there are too few simulations of each model to clearly identify which. It is also found that an observed strong multi-decadal correlation between jet strength and NAO since the mid-19th century may be specific to this period.

Plain Language Summary

The dominant pattern in sea-level pressure variability over the North Atlantic is the North Atlantic Oscillation (NAO), which is strongly associated with climate variations over western Europe. However, major focus of current research is that climate models broadly do not reproduce large enough low-frequency (longer than 30 years) NAO variability, with the implication that significant improvements in the skill of decadal weather prediction are possible.

Motivated by this, we analyzed data from 44 of the world's leading models and delved more deeply into major underlying characteristics of low-frequency winter NAO variability, specifically: (1) strength and (2) latitude of the belt of prevailing westerly winds that blow across the North Atlantic from the Eastern USA to Western Europe. Our study revealed that it is the strength of the westerlies, rather than latitude, which underlies models' difficulty in reproducing low-frequency NAO variability.

This more detailed picture also really matters in terms of impacts on European climate, since a more positive NAO associated mainly with stronger westerlies has different climate impacts compared to one associated mainly with more poleward westerlies. This is emphasized by a further finding that either component of the westerlies can dominate NAO variability across different decades and even centuries.

1 Introduction

It is important to understand low-frequency variability of the North Atlantic (NA) climate system since it exerts a strong influence on European climate (Sutton et al., 2018). This is highly relevant to both decadal predictability of future change as well as efforts to improve detection and attribution of climate trends that have occurred in the past. Recent studies have highlighted that a large proportion of contemporary climate models exhibit weak multi-decadal 20th century NA climate variability when compared to observations (Cheung et al., 2017; Han et al., 2016; Kravtsov, 2017; Wang et al., 2017; Zhang & Wang, 2013). Further, many models exhibit weaker-than-observed links between the NAO and low-frequency phenomena such as Atlantic multi-decadal variability (AMV) (Ba et al., 2014; Keeley et al., 2012; Kim et al., 2018; Omrani et al., 2014; Peings et al., 2016). These studies suggest that multi-decadal internal variability of

the NAO is in fact too weak in most contemporary climate models (Kim et al., 2018; Kravtsov, 2017). However, the roles of different drivers associated with both internal variability and external forcing remain unclear. For example there are still questions over possible drivers of the dramatic increase in the winter NAO during the 30-year period between the 1960s and 1990s.

Recent research shows that diagnostics of the regional NA eddy-driven tropospheric westerly jet can help to improve understanding of key drivers and impacts of NAO variability. Woollings et al. (2015) found that 20th century inter-annual winter NAO variability is largely associated with variability in jet latitude whereas multi-decadal NAO variability (> 30 years) is more strongly related to variability in jet strength. To illustrate the importance of this, Figure 1 shows the climatological winter-mean lower-tropospheric westerly wind structure of the NA region, for which a basin-wide (~60°W to ~0°E) strengthening and/or poleward shifting of the mid-latitude wind maximum (the jet) are both associated with a more positive NAO (note that only the shorter-term linkage is shown here and the interested reader is referred to Woollings et al. (2015) for an in-depth evaluation of such relationships at different timescales). A key point is that for a given change in the NAO the impacts or drivers of that change depend strongly on the ratio of associated jet shifting and/or strengthening, which exhibit contrasting spatial correlation patterns with local westerly wind across the NA and over Europe (compare Figures 1b and 1c). The above-mentioned multi-decadal winter jet strength variability exhibits a distinct maximum in power at low frequencies that is strongly correlated with AMV (Woollings et al., 2014). However, for jet latitude there is no such low-frequency maximum in winter variability. Furthermore, idealized model experiments produce different sensitivities of jet latitude and strength to different external drivers (Baker et al., 2017; McGraw & Barnes, 2016).

These studies motivate us to carry out an analysis of NA jet variability across the CMIP5 models to help to identify reasons for the relatively weak simulated low-frequency NAO variability. We additionally utilize the large ensemble size of the CMIP5 simulations to evaluate the longer-term stationarity of the relationships between low-frequency jet and NAO variability, which is important for understanding spatial patterns of impacts on the NA climate system. Our analysis aims to address two research questions:

1. To what extent is the observed low-frequency variability in jet strength reproduced across the CMIP5 historical simulations?

2. Is the observed link between jet strength and the NAO at multi-decadal time-scales reproduced in the CMIP5 simulations?

2 Data and methods

2.1 CMIP5 data

Output from all-forcing historical coupled simulations of the World Climate Research Programme's (WCRP's) Coupled Model Intercomparison Project Phase 5 (CMIP5) was used for this analysis (Taylor et al., 2012). The fields analyzed were mean sea level pressure (MSLP) and zonal wind at the 850 hPa level (U850 hereafter). Ideally daily fields would have been used for the main analysis of U850, but these were generally only archived for the later part of the 20th century in the historical simulations. The sensitivity to this limitation is evaluated using available daily mean fields of U850 and the results are provided later in this section (see Sections 2.4 and

2.6). We analyzed all available realizations (i.e. individual historical simulations) with the above variables and output available back to at least 1861. This comprised 133 members from 46 different models (Supporting Table S1).

2.2 Twentieth Century Reanalysis Version 2c

The NOAA/CIRES Twentieth Century Global Reanalysis Version 2c (20CRv2c) was used to derive estimates of real-world jet variability (Compo et al., 2015). This version of the 20CR range of reanalysis datasets extends back to 1851, but the post-1861 period has been described as more suitable for climate studies and is therefore used here. To provide a measure of uncertainty in the re-analysis-derived results, all 56 ensemble members were evaluated. Decadal variability of the NA jet in 20CR has been found to be similar to that in the century-long ERA20C reanalysis (Woollings et al., 2018).

2.3 NAO indices

Two different NAO indices were used to help ensure robustness of the results and to aid comparison with earlier studies (e.g. Kelley et al., 2012; Osborn, 2004). First, following Scaife et al. (2009), a point index was defined as the non-normalized difference between winter season (December to February; DJF hereafter with the month of January defining the year of each winter) MSLP over the Azores (Ponta Delgada) and Iceland (Akureyri). For the gridded datasets (20CRV2c and CMIP5 output) bilinear interpolation was used to extract MSLP values at these locations. Second, an Empirical Orthogonal Function (EOF)-based approach was also used, defined here as the principal component time series of the leading EOF of winter-mean MSLP anomalies over each reanalysis or CMIP5 time series over the NA region (20-80N, 90W-40E) (following Hurrell, 1995).

2.4 Jet strength and latitude diagnostics

The diagnostics of NA jet strength and latitude in the lower troposphere draw from Woollings et al. (2015), who use U850. For each U850 field (monthly or daily), the longitudinal mean between 60°W and 0° was first calculated at each latitude. This was then used to identify the maximum (jet strength) and its location (jet latitude). Winter averages were then estimated as a mean of the monthly or daily jet diagnostics through DJF. The same diagnostics were applied to both the 20CRv2c and CMIP5 data. Due to a lack of daily-mean data covering the full length of historical CMIP5 simulations, our analysis was conducted based on monthly mean U850 fields. A comparison between available overlapping monthly and daily CMIP5 data suggests that diagnostics based on monthly mean fields are a close analogue for those derived from daily data (see Supporting Information S2 for details).

2.5 Frequency power spectra

Power spectra were generated from unsmoothed time series of winter-mean NAO and jet diagnostics. A common year range of 1862-2005 was used across the CMIP5 model realizations and 20CRv2c for this part of the analysis to ensure comparable frequency bins.

3 Results

Figure 2 (a-d) shows decadally-smoothed time series of winter NAO, jet latitude and jet strength anomalies from all available CMIP5 realizations and ensemble means from 20CRv2c

reanalysis data (see Supporting Information S1 for smoothing methodology). All four observed diagnostics exhibit significant increases over the 1960s-1990s period, which for the NAO indices and jet latitude are the largest in the period evaluated. For jet strength there is a larger 30-year increase during the 1880s-1910s. This coincides with a period of declining AMV index values and is part of the multi-decadal correlation between the AMV and jet strength (Woollings et al., 2015).

From Figure 2 (a-d) there is evidence of contrasting amplitudes of variability in 20CRv2c compared to CMIP5 models. This is particularly the case for jet strength (Figure 2d), for which the standard deviation of the 30-year smoothed de-trended 20CRv2c ensemble mean time series (0.59 m s^{-1}) exceeds the largest standard deviation derived from any of the time series from the 133 CMIP5 historical realizations (0.57 m s^{-1}).

A similar contrast is also evident in terms of extreme 30-year linear trends (Figure 2 (e-h)). The 30-year period 1965-1994 has previously been highlighted as exhibiting a large observed NAO increase, so this trend length was chosen in Figure 2 to compare with the frequency of occurrence in the CMIP5 models. Here maxima in rolling 30-year overlapping trends (starting just one year apart) for each CMIP5 realization are calculated from the decadally-smoothed time series shown in Figure 2 (a-d). The maximum of these overlapping trends is then extracted for each realization and used to populate the histograms shown in Figure 2 (e-h). The same procedure is applied to the decadally-smoothed reanalysis-derived time series and the resulting trends are shown by the vertical lines in Figure 2 (e-h). By this measure, 30-year trends matching or exceeding the largest seen in the 20CRv2c ensemble mean are less likely for jet strength (3.0 standard deviations (std) from the multi-realization mean) than for the NAO indices (2.4 std for the point index and 2.7 std for the EOF index) or jet latitude (1.0 std). Linear de-trending of the time series brings CMIP5 and 20CRv2c maximum jet strength trends marginally closer (2.9 std) due to a small positive long-term trend in the re-analysis-estimated jet strength (see Figure S3).

A more comprehensive evaluation across different timescales is achieved by using power spectra analysis (Figure 3). This allows an examination of the extent to which CMIP5 historical simulations reproduce the reanalysis-derived significant peak in low-frequency spectral power in jet strength identified by Woollings et al. (2014). Figure 3d shows that the observed low-frequency maximum in spectral power of jet strength at approximately 70 years stands out from the 133 historical CMIP5 realizations. The same conclusion, though less clear, can be reached for the NAO indices (Figures 3a,b). For jet latitude however the CMIP5 models broadly overlap the 20CRv2c-derived power spectrum (Figure 3c). Isolating the low-frequency part of the power spectra and displaying the spectral power for each model and realization immediately illustrates the large internal climate variability across different historical realizations (Figure 4). Despite the fact that in many cases historical simulations from the same model produce a wide range of low-frequency power, it is also clear that only a very small number of realizations get close to the magnitude of the observed relative spectral power for jet strength. Note also that CMIP5-reanalysis differences are even more pronounced in the absence of linear de-trending (Figures S4 and S5).

Another key characteristic of the observed NAO is that its low frequency variability is more strongly related to jet strength variability than jet latitude variability (Figure 5) (Woollings et al., 2015). However, here we found that the opposite is seen across the CMIP5 ensemble, with on average a higher correlation between 30-yr smoothed jet latitude and NAO time series (r =

191 0.66 for point index and 0.68 for EOF index) than for jet strength vs NAO (r = 0.37 for point
192 index and 0.30 for EOF index. Note that for jet strength vs jet latitude, the CMIP5 models are
193 consistent with 20CRv2c in exhibiting no significant correlation (r = 0.04). With regard to NAO
194 vs jet strength, it remains unclear whether the contrast between models and reanalysis is due to
195 sampling uncertainty of the real world and/or structural biases in the CMIP5 models. The former
196 cannot be discounted since models with a large number of realizations exhibit a wide range of
197 low-frequency correlations over the historical period (Figure 5). This suggests that the high
198 correlation between jet strength and NAO indices evident in reanalyses may be specific to the
199 observational period and not necessarily representative of longer-term behavior.

200 **4 Conclusions**

201 This paper was motivated by recent studies highlighting an apparent lack of multi-
202 decadal NAO variability across contemporary climate models (Kim et al., 2018; Kravtsov, 2017)
203 and the recognition that winter multi-decadal variability appears from reanalyses/observations to
204 be expressed more strongly in North Atlantic (NA) jet strength (Woollings et al., 2015). We have
205 extended previous assessments of NAO variability in multi-model ensembles and included NA
206 westerly jet strength and latitude in a comparison between multi-decadal variability in reanalysis
207 data and historical simulations of the CMIP5 models.

208 The main result is that observed (reanalysis) post-1862 multi-decadal jet strength
209 variability falls further into the upper tail of the range spanned by CMIP5 historical simulations
210 than multi-decadal NAO variability. Only a very limited subset of CMIP5 models appear to
211 reproduce the observed peak in low-frequency variability. In contrast, jet latitude exhibits no
212 clear contrast between observed and CMIP5 variability. This picture is evident across a range of
213 different diagnostics: simple smoothed time series, maximum rolling 30-year linear trends and
214 power spectra.

215 The reanalysis/CMIP5 differences in jet strength variability are most prominent for
216 periods of approximately 70 years (Figure 3), which is consistent with a link between multi-
217 decadal variability in jet strength and Atlantic Multi-decadal Variability (AMV) that was
218 identified previously by Woollings et al. (2015) (who found a correlation of -0.48 between AMV
219 and multi-decadal jet strength variability using a similar jet strength metric). Studies show that
220 the observed AMV is stronger than that in most CMIP5 models (Cheung et al., 2017; Zhang &
221 Wang, 2013). The comparatively prominent observed low-frequency strength variability
222 compared to CMIP5 is consistent with previous work suggesting a too-weak feedback between
223 AMV and atmospheric variability (Kim et al., 2018; Peings et al., 2016; Wang et al., 2017). For
224 example Kim et al. (2018) found that even with realistic AMV-related SST anomalies used in
225 atmosphere-only simulations, multi-decadal NAO variability in the CAM5 model remains
226 stubbornly weaker than observed. Nevertheless, certain CMIP5 models do exhibit evidence of
227 stronger feedbacks. Two CMIP5 models (GFDL-ESM2G (model 22) and HadGEM2-ES (model
228 30)) were identified by Peings et al. (2016) as producing a clear lagged signal between the NAO
229 and AMV. Both models come from families of models (i.e. GFDL models 20-23 and Met Office
230 Hadley Centre models 29-30) that emerge as producing historical realizations with relatively
231 large multi-decadal variability in jet strength (e.g. Fig. 4). It is worth noting from Figure 4 that
232 there is a large scatter between individual realizations from the same model (i.e. internal climate
233 variability). An implication of this is that for each of these and a number of other CMIP5 models,

the ensemble size could be too small to confidently assert how unusual the observed low-frequency peak in jet strength is.

Overall the above results indicate that the too-weak 20th century multi-decadal variability in the NA jet stream, as identified through the NAO in previous studies, is even more pronounced in terms of the jet strength. In terms of climate impacts, such biases in characteristics and strength of low-frequency jet variability are highly important. This is because compared to jet shifting, jet pulsing (i.e. strengthening and weakening) produces contrasting surface temperature correlation patterns over Europe (e.g. Woollings et al., 2015). In addition, variations in the background strength of the jet would also influence shorter-term seasonal and intra-seasonal jet variability (Hanna et al., 2015; Woollings et al., 2018).

Of further relevance to impacts of atmospheric variability, Figure 5 shows that the observed stronger NAO-jet strength relationship on multi-decadal timescales is not stationary in the CMIP5 models. This raises the possibility that the observed correlation is specific to the post-1862 period. The simulated lack of stationarity in such correlations potentially relates to multi-decadal variability of NAO centers of action that have been identified in re-analysis datasets covering the modern era (Moore et al., 2013; Wang et al., 2012), longer-term proxy reconstructions, and climate models (Raible et al., 2006; Raible et al., 2014). As such, multi-decadal NAO variability across different centuries could exhibit contrasting characteristics and impacts. For a shorter-term example, compare the observed positive NAO trends in the periods 1880-1910 and 1960-1990 (Figure 2). The latter of these arose from a combination of jet latitude and strength trends which were not exceptional in themselves. In contrast, the earlier period was linked to an exceptional jet strength trend, potentially associated with the more sustained decline in AMV indices during this period (e.g. Peings et al., 2016). More broadly this study highlights the importance of taking a comprehensive approach to evaluating large-scale NA atmospheric variability, such as the combination of NAO and jet diagnostics presented here or more detailed diagnostics of NAO structure such as the NAO angle index of Wang et al. (2012). Ultimately, such analyses should be used to help inform studies aiming to identify the key physical mechanisms to explain model-observation differences in low-frequency NA climate variability.

Acknowledgments

TB and HL were supported as part of the NERC ACSIS project (NE/N018028/1). TW was supported by the NERC IMPETUS project (NE/L01047X/1). RE was supported by the Met Office Hadley Centre Climate Programme (GA01101). We acknowledge the WCRP's Working Group on Coupled Modelling, which is responsible for CMIP, and we thank the climate modeling groups (listed in Table S1 of this paper) for producing and making available their model output. For CMIP the U.S. Department of Energy's Program for Climate Model Diagnosis and Intercomparison provided the coordinating support and led development of software infrastructure in partnership with the Global Organization for Earth System Science Portals. CMIP5 data can be accessed at https://esgf-node.llnl.gov/projects/cmip5/. The 20CRv2c data was provided by the NOAA/OAR/ESRL PSD, Boulder, Colorado, USA from their Web site at https://www.esrl.noaa.gov/psd/. Support for the 20CRv2c dataset is provided by the U.S. Department of Energy, Office of Science Biological and Environmental Research (BER), and by the National Oceanic and Atmospheric Administration Climate Program Office.

References

Ba, J., Keenlyside, N. S., Latif, M., Park, W., Ding, H., Lohmann, K., et al. (2014). A multi-model comparison of Atlantic multidecadal variability. *Clim. Dyn., 43*(9-10), 2333-2348. doi:10.1007/s00382-014-2056-1

Baker, H. S., Woollings, T., & Mbengue, C. (2017). Eddy-Driven Jet Sensitivity to Diabatic Heating in an Idealized GCM. *J. Clim., 30*(16), 6413-6431. doi:10.1175/jcli-d-16-0864.1

Cheung, A. H., Mann, M. E., Steinman, B. A., Frankcombe, L. M., England, M. H., & Miller, S. K. (2017). Comparison of Low-Frequency Internal Climate Variability in CMIP5 Models and Observations. *J. Clim., 30*(12), 4763-4776. doi:10.1175/jcli-d-16-0712.1

Compo, G. P., Whitaker, J. S., Sardeshmukh, P. D., Allan, R. J., McColl, C., Yin, X., et al. (2015). NOAA/CIRES Twentieth Century Global Reanalysis Version 2c. Boulder, CO: Research Data Archive at the National Center for Atmospheric Research, Computational and Information Systems Laboratory.

Han, Z., Luo, F. F., Li, S. L., Gao, Y. Q., Furevik, T., & Svendsen, L. (2016). Simulation by CMIP5 models of the atlantic multidecadal oscillation and its climate impacts. *Adv. Atmos. Sci., 33*(12), 1329-1342. doi:10.1007/s00376-016-5270-4

Hanna, E., Cropper, T. E., Jones, P. D., Scaife, A. A., & Allan, R. (2015). Recent seasonal asymmetric changes in the NAO (a marked summer decline and increased winter variability) and associated changes in the AO and Greenland Blocking Index. *Int. J. Climatol., 35*(9), 2540-2554. doi:10.1002/joc.4157

Hurrell, J. W. (1995). Decadal trends in the North-Atlantic oscillation - regional temperatures and precipitation. *Science, 269*, 676-679.

Keeley, S. P. E., Sutton, R. T., & Shaffrey, L. C. (2012). The impact of North Atlantic sea surface temperature errors on the simulation of North Atlantic European region climate. *Q. J. Roy. Meteorol. Soc., 138*(668), 1774-1783. doi:10.1002/qj.1912

Kelley, C., Ting, M. F., Seager, R., & Kushnir, Y. (2012). The relative contributions of radiative forcing and internal climate variability to the late 20th Century winter drying of the Mediterranean region. *Clim. Dyn., 38*(9-10), 2001-2015. doi:10.1007/s00382-011-1221-z

Kim, W. M., Yeager, S., Chang, P., & Danabasoglu, G. (2018). Low-Frequency North Atlantic Climate Variability in the Community Earth System Model Large Ensemble. *J. Clim., 31*, 787-813. doi:10.1175/jcli-d-17-0193.1

Kravtsov, S. (2017). Pronounced differences between observed and CMIP5-simulated multidecadal climate variability in the twentieth century. *Geophys. Res. Lett., 44*(11), 5749-5757. doi:10.1002/2017gl074016

McGraw, M. C., & Barnes, E. A. (2016). Seasonal Sensitivity of the Eddy-Driven Jet to Tropospheric Heating in an Idealized AGCM. *J. Clim., 29*(14), 5223-5240. doi:10.1175/jcli-d-15-0723.1

Moore, G. W. K., Renfrew, I. A., & Pickart, R. S. (2013). Multidecadal Mobility of the North Atlantic Oscillation. *J. Clim., 26*(8), 2453-2466. doi:10.1175/jcli-d-12-00023.1

Omrani, N. E., Keenlyside, N. S., Bader, J., & Manzini, E. (2014). Stratosphere key for wintertime atmospheric response to warm Atlantic decadal conditions. *Clim. Dyn., 42*(3-4), 649-663. doi:10.1007/s00382-013-1860-3

Osborn, T. J. (2004). Simulating the winter North Atlantic Oscillation: the roles of internal variability and greenhouse gas forcing. *Clim. Dyn., 22*(6-7), 605-623. doi:10.1007/s00382-004-0405-1

Peings, Y., Simpkins, G., & Magnusdottir, G. (2016). Multidecadal fluctuations of the North Atlantic Ocean and feedback on the winter climate in CMIP5 control simulations. *J. Geophys. Res.-Atmos., 121*(6), 2571-2592. doi:10.1002/2015jd024107

Raible, C. C., Casty, C., Luterbacher, J., Pauling, A., Esper, J., Frank, D. C., et al. (2006). Climate variability-observations, reconstructions, and model simulations for the Atlantic-European and Alpine region from 1500-2100 AD. *Clim. Change, 79*(1-2), 9-29. doi:10.1007/s10584-006-9061-2

Raible, C. C., Lehner, F., Gonzalez-Rouco, J. F., & Fernandez-Donado, L. (2014). Changing correlation structures of the Northern Hemisphere atmospheric circulation from 1000 to 2100 AD. *Clim. Past, 10*(2), 537-550. doi:10.5194/cp-10-537-2014

Scaife, A. A., Kucharski, F., Folland, C. K., Kinter, J., Bronnimann, S., Fereday, D., et al. (2009). The CLIVAR C20C project: selected twentieth century climate events. *Clim. Dyn., 33*(5), 603-614. doi:10.1007/s00382-008-0451-1

Sutton, R. T., McCarthy, G. D., Robson, J., Sinha, B., Archibald, A., & Gray, L. J. (2018). Atlantic Multi-decadal Variability and the UK ACSIS programme. *Bull. Am. Meteorol. Soc.*, in press. doi:10.1175/bams-d-16-0266.1

Taylor, K. E., Stouffer, R. J., & Meehl, G. A. (2012). An Overview of CMIP5 and the Experiment Design. *Bull. Am. Meteorol. Soc., 93*, 485–498. doi:10.1175/bams-d-11-00094.1

Wang, X. F., Li, J. P., Sun, C., & Liu, T. (2017). NAO and its relationship with the Northern Hemisphere mean surface temperature in CMIP5 simulations. *J. Geophys. Res.-Atmos., 122*(8), 4202-4227. doi:10.1002/2016jd025979

Wang, Y. H., Magnusdottir, G., Stern, H., Tian, X., & Yu, Y. (2012). Decadal variability of the NAO: Introducing an augmented NAO index. *Geophys. Res. Lett., 39*. doi:10.1029/2012gl053413

Woollings, T., Barnes, E., Hoskins, B., Kwon, Y.-O., Lee, R. W., Li, C., et al. (2018). Daily to decadal modulation of jet variability. *J. Clim., 31*, 1297-1314. doi:10.1175/jcli-d-17-0286.1

Woollings, T., Czuchnicki, C., & Franzke, C. (2014). Twentieth century North Atlantic jet variability. *Q. J. Roy. Meteorol. Soc., 140*(680), 783-791. doi:10.1002/qj.2197

Woollings, T., Franzke, C., Hodson, D. L. R., Dong, B., Barnes, E. A., Raible, C. C., et al. (2015). Contrasting interannual and multidecadal NAO variability. *Clim. Dyn., 45*(1-2), 539-556. doi:10.1007/s00382-014-2237-y

Zhang, L. P., & Wang, C. Z. (2013). Multidecadal North Atlantic sea surface temperature and Atlantic meridional overturning circulation variability in CMIP5 historical simulations. *J. Geophys. Res. - Oceans, 118*(10), 5772-5791. doi:10.1002/jgrc.20390

Figure Captions

Figure 1. Reanalysis (20CRv2c) climatological (1861-2014) winter-mean U850 (line countours) and regression slopes (color fill) of time series of winter-mean U850 at each grid point on (**a**) NAO point index, (**b**) jet latitude and (**c**) jet strength. For the U850 climatologies, solid (dashed) contour lines denote positive (negative) values with levels -9, -6, -3, 0, 3, 6, 9 m s^{-1}. All time series were linearly de-trended prior to calculation of regression slopes.

Figure 2. Panels **a-d** show smoothed time series of winter NAO point index, NAO EOF-based index, jet latitude and jet strength anomalies respectively, with CMIP5 ensemble members shown by decadally-smoothed thin grey lines and the 20CRv2c ensemble mean shown by the thick black lines (dashed shows decadally-smoothed time series and dotted shows 30-year smoothing). The solid segments of the decadally-smoothed 20CRv2c time series highlight periods containing the maximum 30-year linear trend. All available years are shown from each time series, hence the differing start and end dates in some cases. Panels **e-h** show histograms of maximum 30-year linear trends of the smoothed and de-trended CMIP5 time series shown in panels **a-d**. Vertical black lines show maximum 30-year linear trends from each of the 20CRv2c ensemble members (i.e. trends during the periods highlighted by solid black lines in **a-d**).

Figure 3. Proportional power spectral density (i.e. divided by the mean across all frequency components) of (**a**) NAO point index, (**b**) NAO EOF index, (**c**) jet latitude and (**d**) jet strength. The grey lines denote individual CMIP5 realizations and the black lines show 20CRv2c ensemble members. Each time series was linearly de-trended prior to the spectral analysis and the time range was restricted to the common period of 1862-2005 for comparison of the same frequency bins. The dashed line indicates the $p = 0.05$ threshold for the significance of a peak in any particular frequency bin using Fisher's *g*-statistic. In (**d**), the mean p-value across the 56 20CRv2c ensemble members is 0.038 in the 72-year period bin.

Figure 4. Low-frequency proportional power (mean over periods of between 40 to 100 years of results shown in Figure 3) for (**a**) NAO point index, (**b**) NAO EOF index, (**c**) jet latitude and (**d**) jet strength. The grey horizontal lines show the values calculated from 20CRv2c ensemble members. Each asterisk represents one historical CMIP5 realization arranged into columns for each model (see supporting Table S1 for model names).

Figure 5. Correlation coefficients of 30-year smoothed time series of NAO point index vs (**a**) jet latitude and (**b**) jet strength. As in Figure 4 each CMIP5 historical realization is indicated by an asterisk and the 20CRv2c reanalysis ensemble members by the horizontal solid grey lines. See Figure S6 for a version based on the EOF-based NAO index.

Fig. 1

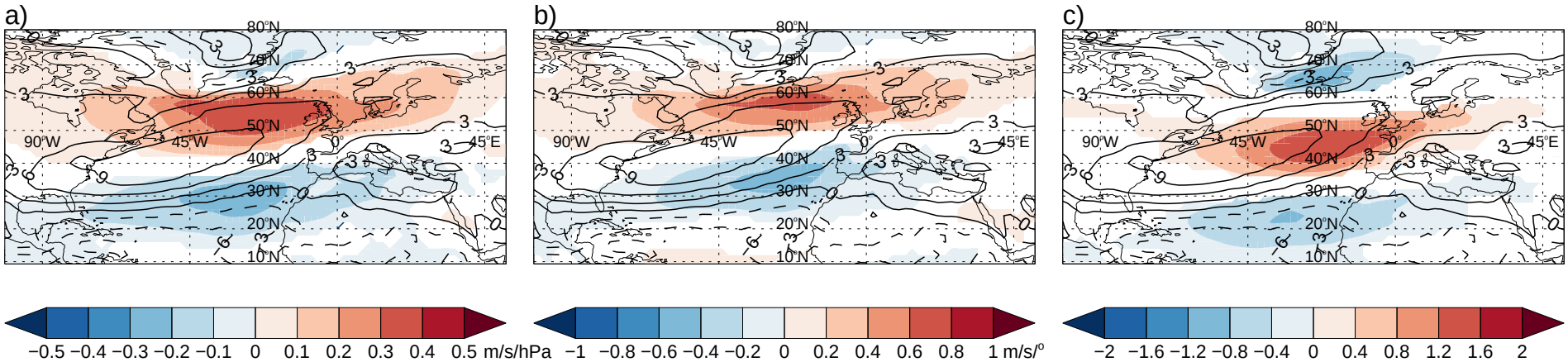
a)
b)
c)
80°N
70°N
60°N
50°N
40°N
30°N
20°N
10°N
90°W
45°W
0°
45°E
−0.5 −0.4 −0.3 −0.2 −0.1 0 0.1 0.2 0.3 0.4 0.5 m/s/hPa
−1 −0.8 −0.6 −0.4 −0.2 0 0.2 0.4 0.6 0.8 1 m/s/°
−2 −1.6 −1.2 −0.8 −0.4 0 0.4 0.8 1.2 1.6 2

Fig. 2

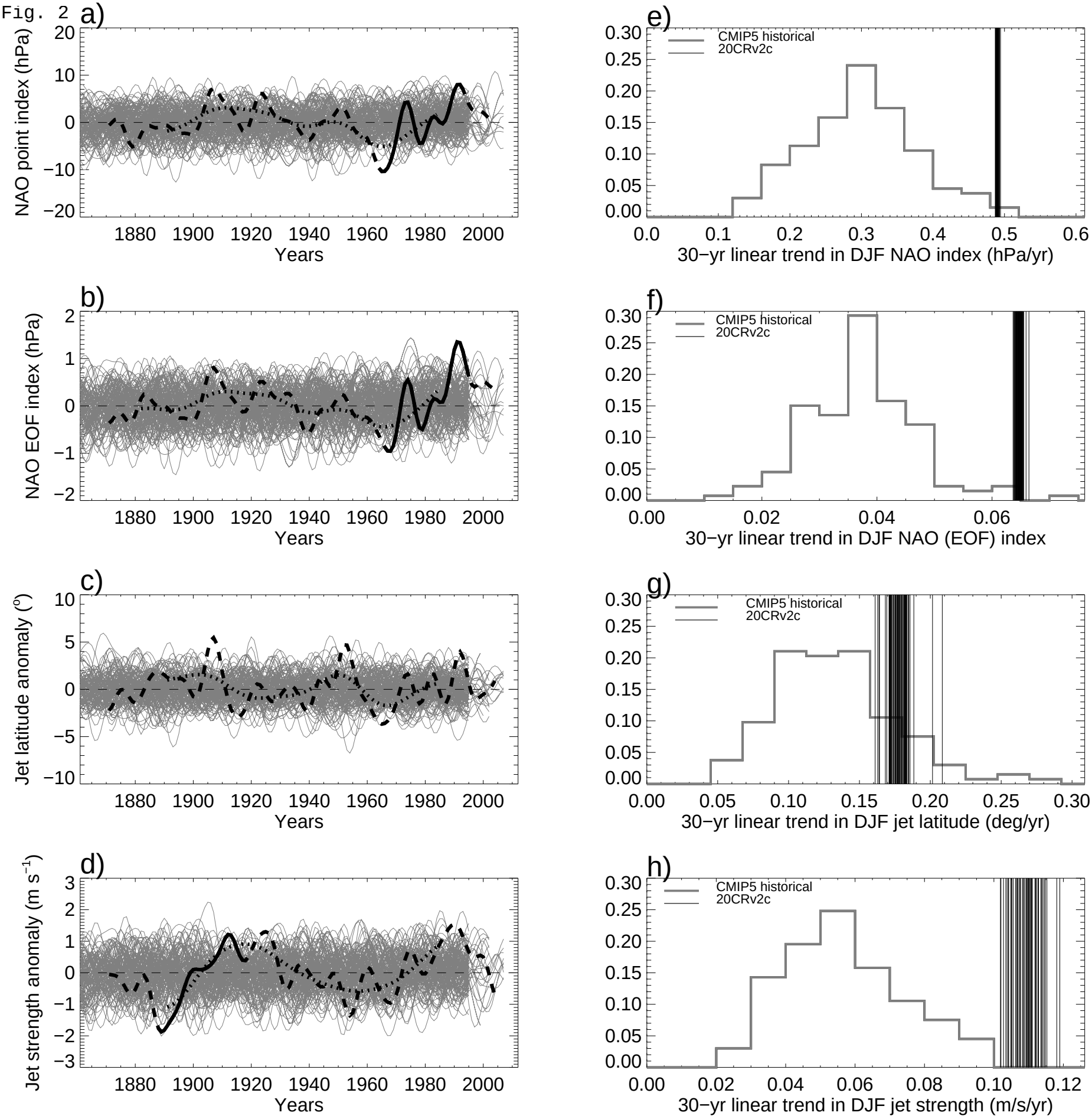
a)
NAO point index (hPa)
Years
b)
NAO EOF index (hPa)
Years
c)
Jet latitude anomaly (°)
Years
d)
Jet strength anomaly (m s−1)
Years
e)
CMIP5 historical
20CRv2c
30−yr linear trend in DJF NAO index (hPa/yr)
f)
CMIP5 historical
20CRv2c
30−yr linear trend in DJF NAO (EOF) index
g)
CMIP5 historical
20CRv2c
30−yr linear trend in DJF jet latitude (deg/yr)
h)
CMIP5 historical
20CRv2c
30−yr linear trend in DJF jet strength (m/s/yr)

Fig.3 a)

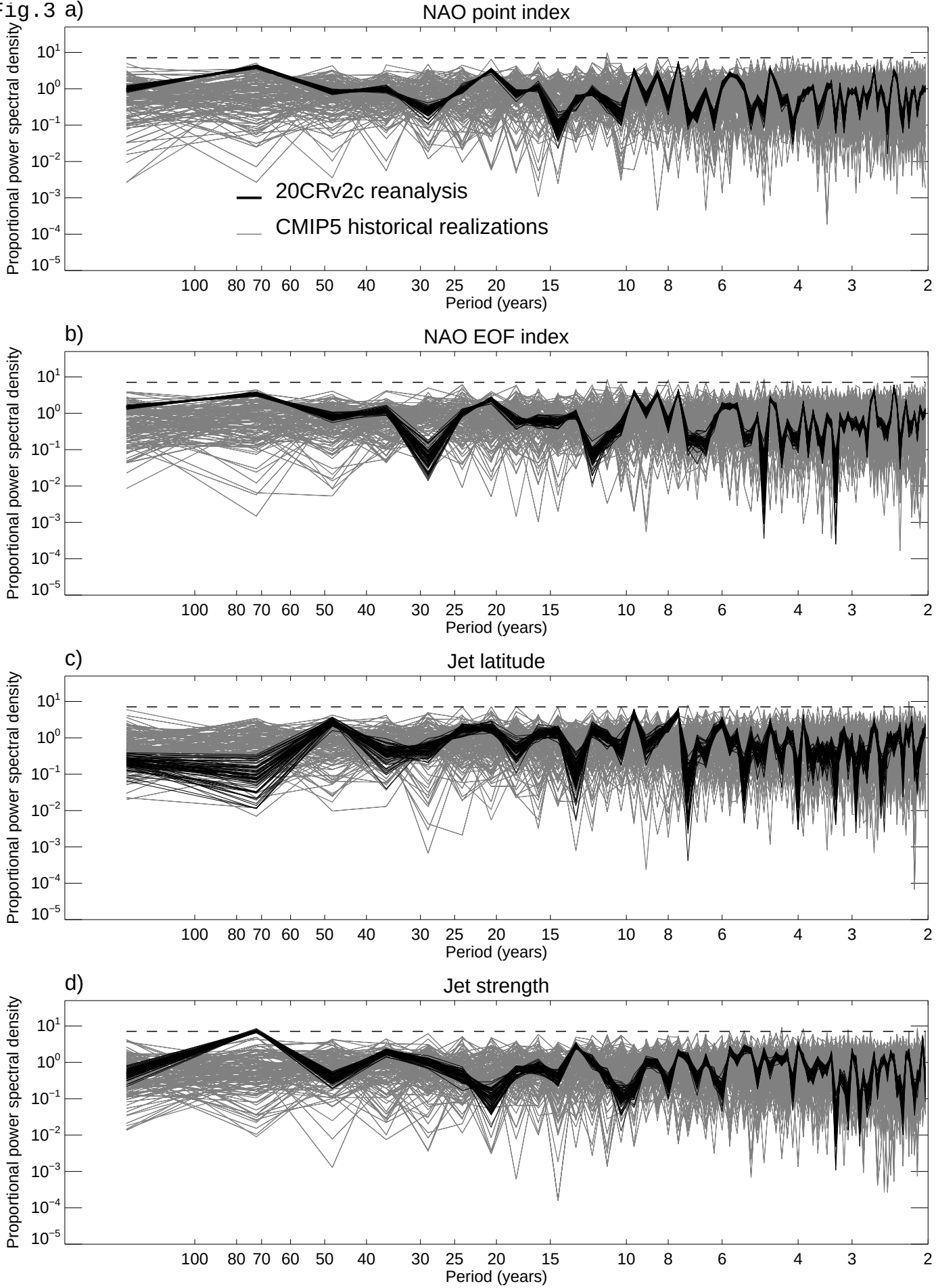
NAO point index
Proportional power spectral density
20CRv2c reanalysis
CMIP5 historical realizations
Period (years)
b)
NAO EOF index
Proportional power spectral density
Period (years)
c)
Jet latitude
Proportional power spectral density
Period (years)
d)
Jet strength
Proportional power spectral density
Period (years)

Fig.4

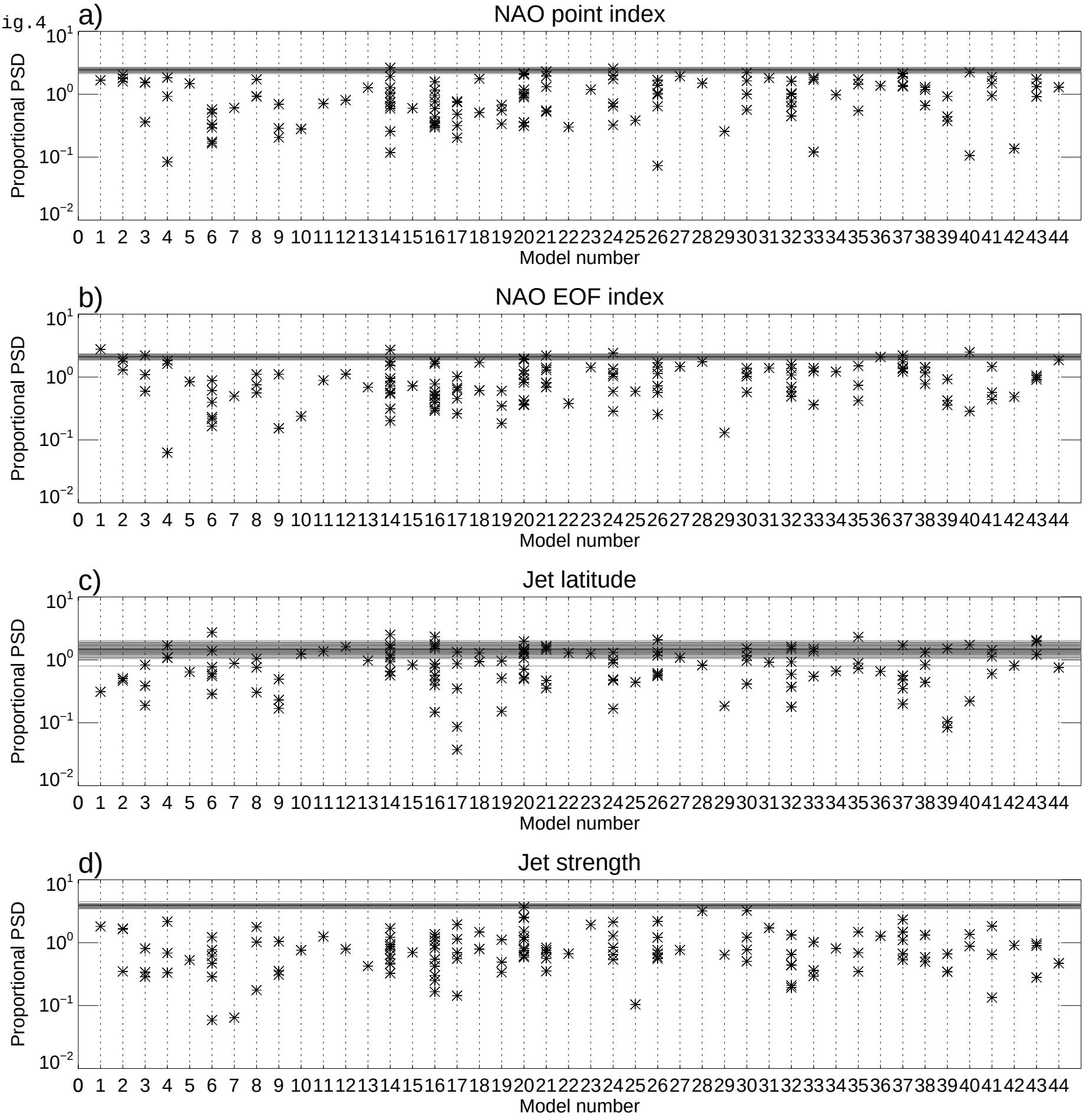
a)
NAO point index
b)
NAO EOF index
c)
Jet latitude
d)
Jet strength
Proportional PSD
Model number

Fig. 5

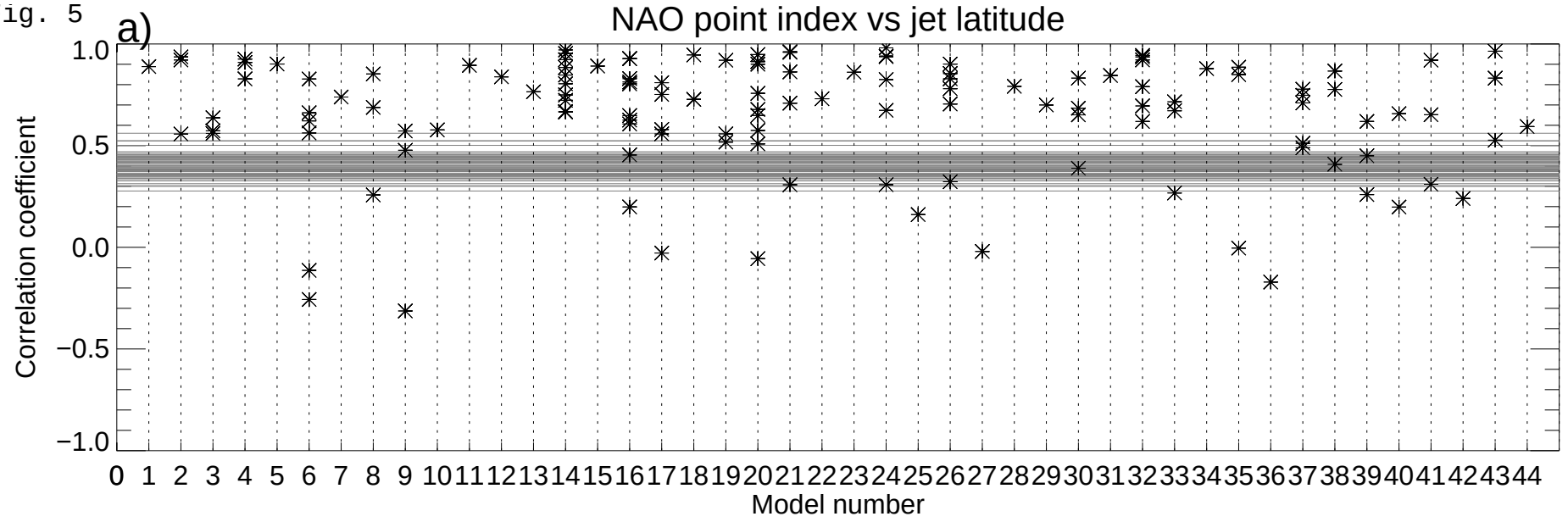
a)
NAO point index vs jet latitude
Correlation coefficient
1.0
0.5
0.0
−0.5
−1.0
0 1 2 3 4 5 6 7 8 9 10 11 12 13 14 15 16 17 18 19 20 21 22 23 24 25 26 27 28 29 30 31 32 33 34 35 36 37 38 39 40 41 42 43 44
Model number

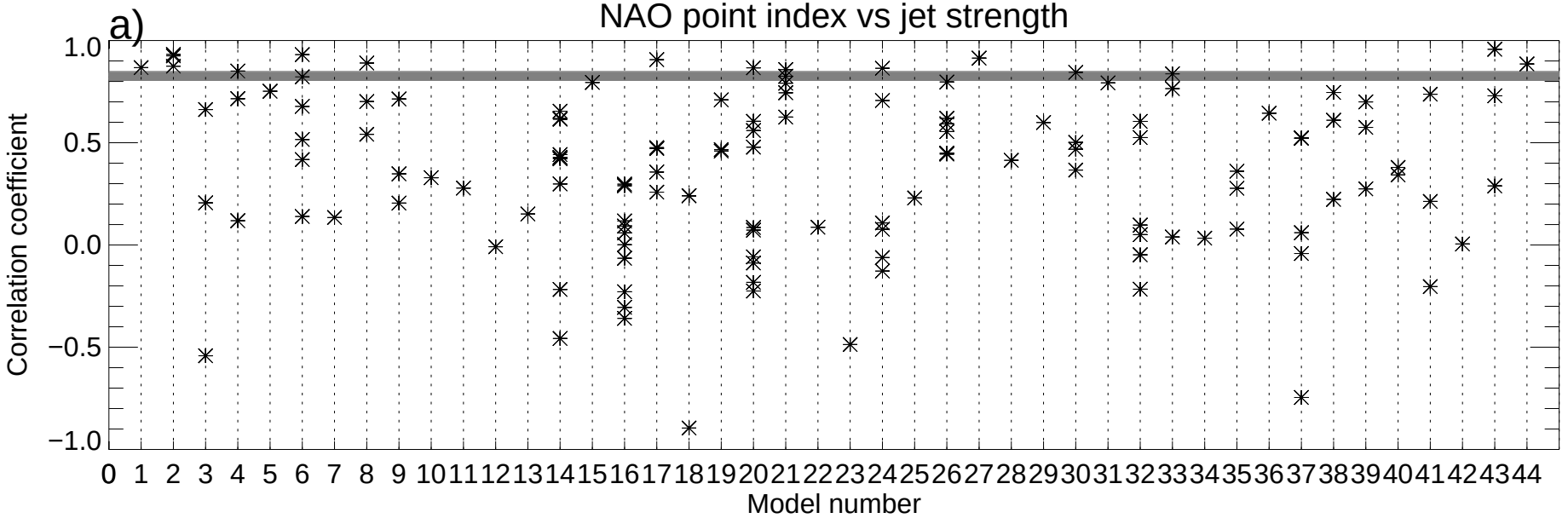
a)
NAO point index vs jet strength
Correlation coefficient
1.0
0.5
0.0
−0.5
−1.0
0 1 2 3 4 5 6 7 8 9 10 11 12 13 14 15 16 17 18 19 20 21 22 23 24 25 26 27 28 29 30 31 32 33 34 35 36 37 38 39 40 41 42 43 44
Model number